

GINGA OBSERVATION OF AN AM HERCULIS TYPE SOURCE H0538 + 608

M. ISHIDA,¹ A. SILBER,² H. V. BRADT,² R. A. REMILLARD,² K. MAKISHIMA,¹ AND T. OHASHI¹

Received 1990 February 12; accepted 1990 July 17

ABSTRACT

Results from a *Ginga* observation of the AM Her type object, H0538 + 608, carried out on 1988 February 7–10, are presented. During the first half of the observation (pulsing state) the source showed periodic modulations caused by the white dwarf rotation, and the modulation profile was characterized by a flat top and a flat bottom. During the second half, the source was in a remarkable flaring state and the periodic modulation disappeared. The dramatic change of the X-ray light curve is interpreted in terms of a change of accretion pattern between an eclipsing spot and a noneclipsing spot. The phase determined by the X-ray data coincides well with that expected from the optical polarimetry data by Mason *et al.*, providing strong support for their tentative precise ephemeris.

The spectrum is well described throughout by a thin thermal model including an iron K-line with equivalent width of some hundred eV, supporting the standard model for the hard X-ray emission region. The temperature in the pulsing state was found to change with the spin phase of the white dwarf. In the flaring state, the temperature showed a positive correlation with the source luminosity.

Subject headings: stars: accretion — stars: individual (H0538 + 608) — stars: white dwarfs — X-rays: binaries

I. INTRODUCTION

The AM Her type sources are cataclysmic variables containing a late type star and a strongly magnetized ($\sim 10^7$ G) white dwarf (Cropper 1990). The dipole magnetic field of the white dwarf is so strong that the spin of the white dwarf is synchronized to the orbital motion of the binary system. The strong magnetic field controls mass flow from the optical counterpart to either one or both magnetic poles of the white dwarf, and a standing shock is formed near the surface. Below the shock, the kinetic energy of the flow is converted into thermal energy, producing strong hard X-ray emission. In general these sources are observed as “white dwarf pulsars,” for the dipole axis of the white dwarf is usually tilted with respect to the spin axis.

As pointed out by Lamb (1985), there are three important emission mechanisms in AM Her type sources: (1) optical cyclotron emission originating from the accretion column; (2) optically thick UV to soft X-ray emission (with a temperature of 20–50 eV, usually approximated by blackbody radiation) from the white dwarf surface; and (3) optically thin hard X-ray emission (with a temperature of a few times 10 keV) from the postshock hot region. It is not yet clear, however, how gravitational energy of the accreting matter is distributed among these three components. For example, if blackbody emission from the white dwarf surface is reprocessed emission from the other two mechanisms, its luminosity should be of the same order as the total power of the other two from a simple geometrical consideration, namely $L_{\text{bb}} \sim L_{\text{br}} + L_{\text{cyc}}$. But observations of AM Her type sources indicate that $L_{\text{bb}} = (1-50) \times (L_{\text{br}} + L_{\text{cyc}})$ (Lamb 1985 and references therein). This is the so-called soft excess problem. For a better understanding of the emission mechanism in AM Her type sources, knowledge of the hot plasma in the postshock region is necessary. For this purpose, hard-X ray spectroscopy is essential.

The X-ray source H0538 + 608 was detected by *Uhuru* and the *HEAO 1* LASS (Large Area Sky Survey) and cataloged as

4U 0541 + 60 (Forman *et al.* 1978) and 1H 0533 + 607 (Wood *et al.* 1984), respectively. The 2–10 keV X-ray flux of this source is exceeded only by two others of the same type (AM Her itself and EF Eri).

Remillard *et al.* (1986) optically identified this source as a star with $B \sim 15$. They pointed out that H0538 + 608 was in a low state ($B \geq 17$) in 1934 and 1939. Such a low state is a common property among cataclysmic variables. In addition, the source showed other characteristics that are common to AM Her type sources, including 10% circular polarization, strongly modulated brightness variation, and intense flickerings on time scales of seconds. They also found that the energy flux in an optical band (300–700 nm) is 2×10^{-11} ergs cm^{-2} s^{-1} , and the rotation period of the white dwarf is 3.1 ± 0.2 hr based on optical polarimetry. Recently, Mason, Liebert and Schmidt (1989) performed long-term optical polarimetry that yielded a refined rotation period of 3.331 ± 0.015 hr, despite strong aperiodic behavior.

In the UV band (Bonnet-Bidaud and Mouchet 1987), the 120–320 nm flux is 2.6×10^{-11} ergs cm^{-2} s^{-1} , and the spectrum is characterized by unusual carbon and nitrogen emission lines which are commonly seen in the spectra of old novae.

X-ray observations of H0538 + 608 with *EXOSAT* (Shrader *et al.* 1988) have revealed a number of remarkable characteristics. Soft X-ray eclipses, confined to X-ray energies below 1 keV, indicate the occultation of the X-ray-emitting region by an accretion stream with a period of 3.30 ± 0.03 hr. Simultaneous X-ray, UV, and optical observations indicate a notable absence of the “soft excess” which characterizes other AM Her systems. Even more striking, however, is the chaotic appearance of the X-ray light curves from the Medium Energy (ME) experiment (1–8 keV). The X-ray intensity surges were as large as a factor ~ 6 , on a time scale ~ 1 hr. There were no apparent changes in the X-ray spectrum, although the ME detector could only set a lower limit on the temperature; $kT \geq 23$ keV (90% confidence limit). The unstable behavior in the X-ray and optical (Silber *et al.* 1990) light curves and in the optical polarimetry suggests the possibility of asynchronous rotation such as

¹ Department of Physics, Faculty of Science, University of Tokyo.

² Center for Space Research, Massachusetts Institute of Technology.

TABLE 1
JOURNAL OF OBSERVATIONS

Date of Observation (1988 UT)	Mode	Time Resolution (s)
Feb 7 18:09–Feb 8 1:00	MPC-1	4, or 0.5
Feb 8 1:30–Feb 8 16:25	MPC-1	16
Feb 8 16:26–Feb 8 23:25	MPC-1	4, or 0.5
Feb 8 23:26–Feb 9 16:32	MPC-1	16
Feb 9 16:32–Feb 9 23:31	MPC-1	4, or 0.5
Feb 10 0:30–Feb 10 16:32	MPC-1	16

that detected in V1500 Cyg (Stockman, Schmidt, and Lamb 1988).

To further study these unexplained phenomena, H0538 + 608 was observed with the *Ginga* X-ray astronomy satellite which has good sensitivity in the 2–37 keV band, along with simultaneous optical coverage which will be published elsewhere. In this paper, we present the X-ray results and discuss the state of the hot plasma and the system parameters based on these results.

II. OBSERVATIONS

The *Ginga* observations were carried out over 3 days, 1988 February 7–10, with the LAC experiment (Large Area proportional Counter: Turner *et al.* 1989) on board the *Ginga* satellite (Makino and the ASTRO-C Team 1987). The background was taken from a nearby sky region on 1988 February 6 and 10. The net on-source time was about 60,000 s (Table 1). Optical observations, including spectroscopy and photometry, were conducted simultaneously at the Michigan-Dartmouth-MIT Observatory on Kitt Peak, and those results as well as comparisons between the X-ray and optical data will be published elsewhere (see Silber *et al.* 1990).

III. DATA ANALYSIS AND RESULTS

a) Light Curve and Spin Modulation

The observed light curve of H0538 + 608 in the 1.8–18.6 keV energy band after background subtraction and aspect correction is shown in Figure 1. Though the data exhibit random variations, the periodic modulation caused by the white dwarf rotation can be seen during the period up to about 12:00 UT on February 9. After that, the data are dominated by erratic variability, and the pulse modulation disappears. The intensity eventually increases by about a factor of 2. Hereafter we divide the data into two groups, before and after 12:00 on February 9, and refer to them as the “pulsing state” and “flaring state,” respectively. The average X-ray luminosity is 9.2×10^{31} ergs s^{-1} in the pulsing state and 1.4×10^{32} ergs s^{-1} in the flaring state in the 1.8–37.4 keV energy band for an assumed distance of 100 pc.

The spin period of the white dwarf is determined to be 3.33 ± 0.05 hr from folds of the pulsing state data, which is consistent with the values quoted above. The folded pulse profile is shown in Figure 2a. We defined our phase origin as the phase of minimum intensity of the narrow H α emission line, namely, 1988 February 8.065. The profile is characterized by a flat top and a flat bottom. Such a flat peak (or bottom) profile has been observed in other AM Her type sources: AM Her itself (Heise *et al.* 1985) and CW 1103 + 254 (Beuermann and Stella 1985). The intensity profile in the flaring state folded with the same period is shown in Figure 2b. The modulation amplitude of ~ 10 counts s^{-1} shown in this figure exceeds the statistical error by a factor of ~ 20 . This modulation, however, is undoubtedly caused by the random variations since the degree of deviations from a flat intensity profile is almost the same for any trial period around the spin period.

b) Average Spectra

The average pulse-height spectra of the pulsing state and the flaring state are shown in Figures 3a and 3b, respectively. We

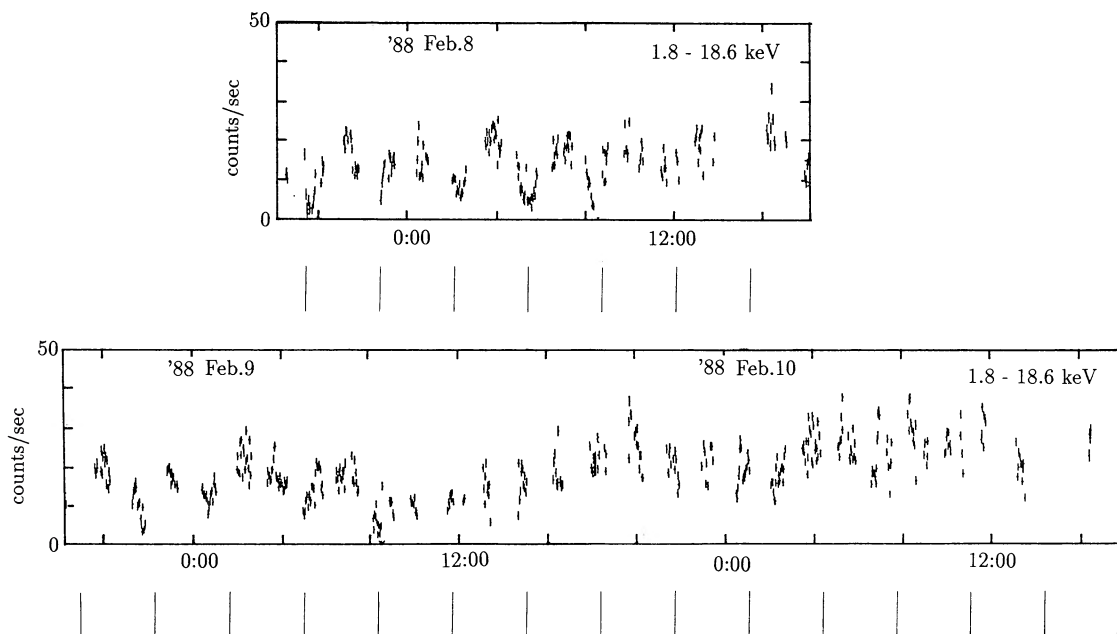


FIG. 1.—The observed light curve of H0538 + 608 in the 1.8–18.6 keV energy band. The periodic feature disappeared at the epoch of 12:00 of 1988 February 9. Tick marks indicate the dip center positions with a period of 3.33 hr.

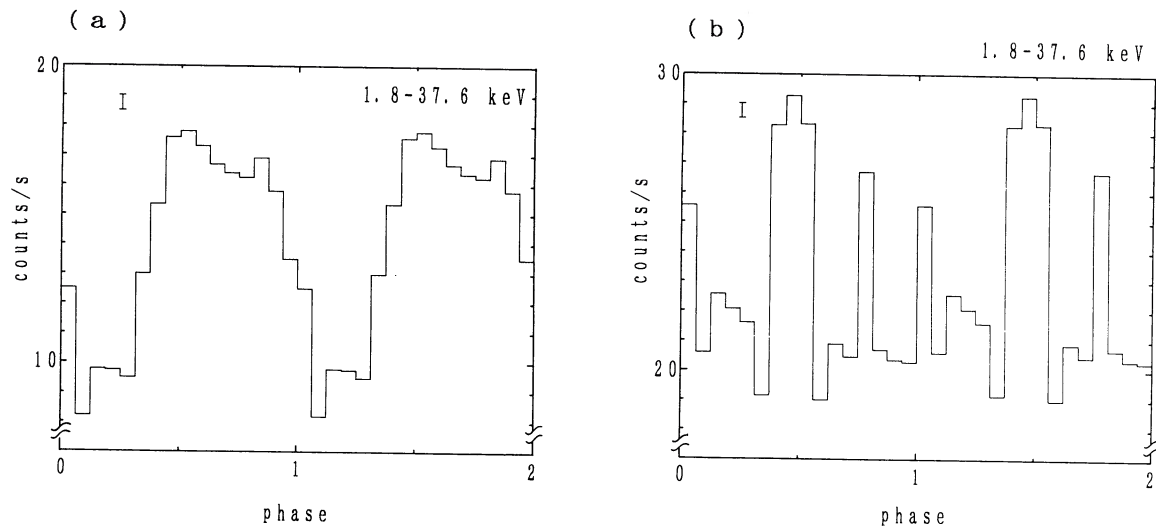


FIG. 2.—The folded light curves of (a) the pulsing state and (b) the flaring state in the 1.8–37.6 keV energy band with a period of 3.33 hr and with the same phase zero epoch of 1988 February 8.065. Also shown are the typical 1σ error for each bin, calculated by the scattering of each datum from the folded light curve. Phase zero of the ephemeris of Mason *et al.* (1989) corresponds to a phase 0.34 ± 0.02 in this figure.

subtracted the model background developed by Hayashida *et al.* (1989). For a cross check of the background subtraction, we also subtracted the measured background in the nearby sky from the on-source data and found that the two results were consistent.

The spectra are fitted with two models: Model 1; thermal bremsstrahlung and iron emission-line with interstellar/circumstellar absorption; and Model 2; power-law and iron emission-line with interstellar/circumstellar absorption. For the thermal bremsstrahlung model, we adopt the Gaunt factor calculated by Gould (1980) which is expected to be accurate within 1% up to a plasma temperature of 10^8 K. For the iron line, we assume a Gaussian shape and treat the line center energy and line intensity as free parameters, whereas the line width is fixed at 0.2 keV which is much narrower than the LAC energy resolution (18% FWHM at 6 keV). For absorption, we assume neutral matter of solar abundance (Morrison and McCammon 1983).

The results of the fitting are summarized in Table 2. Model 1 gives a significantly better fit than model 2 for both spectra. This fact suggests that, in spite of the relatively high value of χ^2

for the pulsing state, the hard X-rays from H0538+608 originate from an optically thin hot plasma with $kT \sim 30$ keV.

c) Phase-resolved Spectra in the Pulsing State

The analysis of the phase resolved spectra in the pulsing state is described here. First, we made two spectra corresponding to the flat top and the flat bottom of the pulse profile. They are shown in Figures 3c and 3d together with the best fit of model 1. The results of the spectral fitting are summarized in Table 3. The luminosities in the 1.8–37.4 keV band are 5.3×10^{31} ergs s^{-1} and 1.3×10^{32} ergs s^{-1} for the flat-bottom and the flat-top phases, respectively, for the assumed distance of 100 pc. The temperatures are ~ 38 keV and ~ 26 keV for the flat-top and flat-bottom phases, respectively.

The fit for the flat-top phase gives a reduced χ^2 value of 1.45 with 26 degrees of freedom, which means the model cannot be rejected at 95% confidence level. The residuals in Figure 3c shows a diplike spectral structure around 10 keV. This structure is likely due to the iron *K*-edge, whose presence is also suggested by the energy of the strong iron emission line (see discussion below). We therefore modify model 1 to include the

TABLE 2
AVERAGE X-RAY SPECTRA

MODEL	TEMPERATURE (keV)	PHOTON INDEX	Fe LINE PARAMETER			log NH	REDUCED χ^2 (DOF)
			Center (keV)	Intensity (counts s^{-1})	EW (eV)		
Pulsing State							
1 ^a	30.0 ± 4.5	...	6.56 ± 0.08	0.35 ± 0.05	340 ± 40	22.0 ± 0.05	1.80 (26)
2 ^b	1.58 ± 0.02	6.59 ± 0.07	0.41 ± 0.05	390 ± 50	22.2 ± 0.04	3.05 (26)
Flaring State							
1 ^a	25.9 ± 4.3	...	6.59 ± 0.10	0.43 ± 0.07	240 ± 40	21.8 ± 0.07	0.81 (26)
2 ^b	1.63 ± 0.02	6.63 ± 0.08	0.53 ± 0.07	290 ± 40	22.1 ± 0.04	3.14 (26)

^a Thermal bremsstrahlung and iron emission line with interstellar/circumstellar absorption.

^b Power law and iron emission line with interstellar/circumstellar absorption.

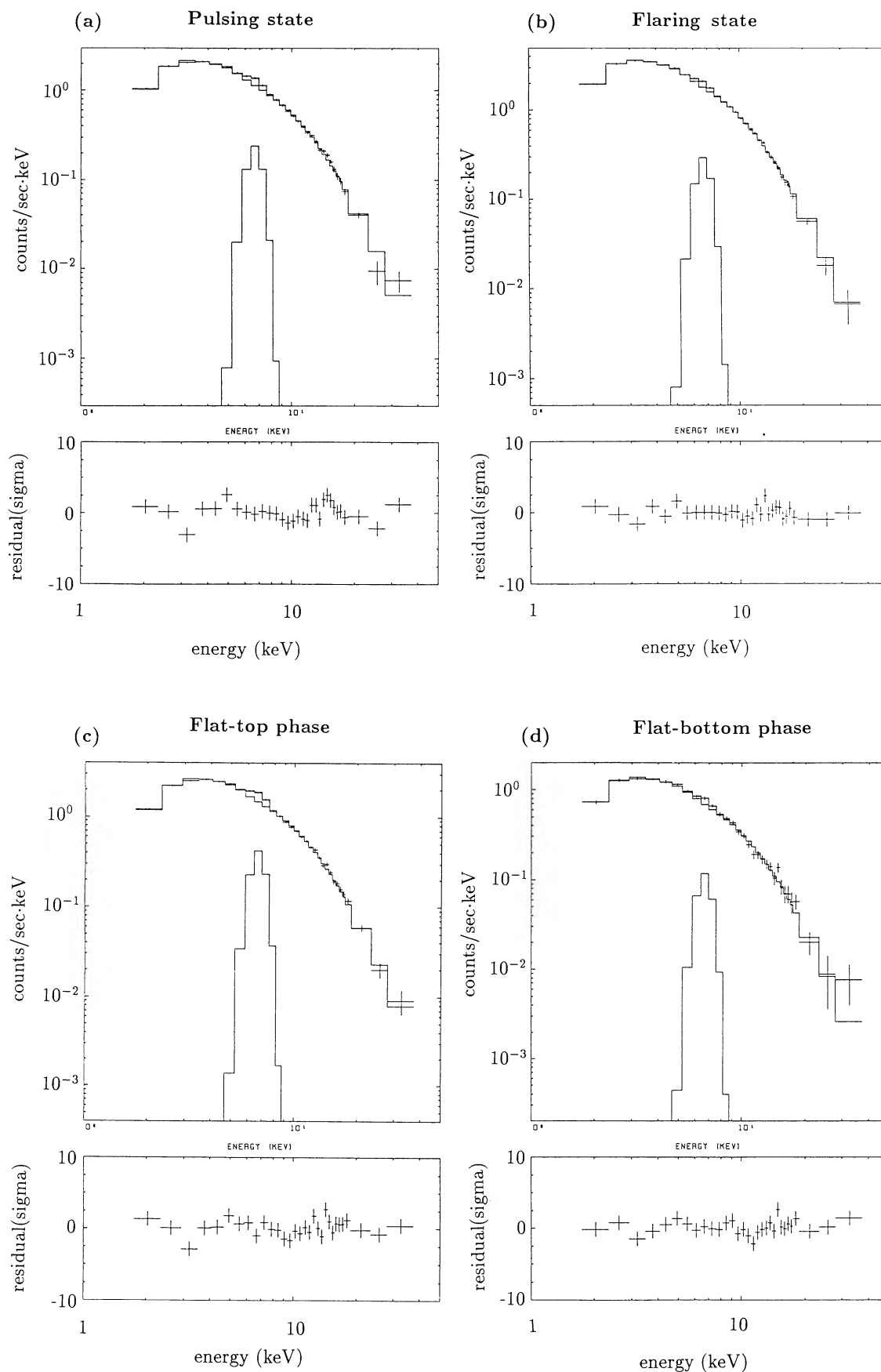


FIG. 3.—Averaged spectrum of (a) the pulsing state, (b) the flaring state, (c) the flat-top phase in the pulsing state, and (d) the flat-bottom phase in the pulsing state. All of them are well fitted with thermal bremsstrahlung models with an iron line. Fitting parameters are listed in Tables 2 and 3.

TABLE 3
X-RAY SPECTRA DURING PULSING STATE

MODEL	TEMPERATURE (keV)	Fe LINE PARAMETER			$\log N_{\text{H}}$	E_{edge} (keV)	$\log N_{\text{Fe}}$	REDUCED χ^2 (DOF)
		Center (keV)	Intensity (counts s ⁻¹)	EW (eV)				
Flat-Top Phase								
1.....	37.6 ± 3.0	6.56 ± 0.06	0.63 ± 0.06	450 ± 50	22.1 ± 0.04	1.45 (26)
3 ^a	41.0 ± 4.1	6.55 ± 0.07	0.58 ± 0.07	410 ± 50	22.2 ± 0.04	8.1 (fixed)	22.9 ± 0.2	1.24 (25)
Flat-Bottom Phase								
1.....	26.2 ± 3.9	6.54 ± 0.25	0.17 ± 0.06	250 ± 100	21.8 ± 0.1	1.00 (26)

^a Thermal bremsstrahlung with iron K-edge and iron emission line with interstellar/circumstellar absorption.

K-edge and try to fit the flat-top phase spectrum. The new model 3 therefore is thermal bremsstrahlung with iron edge and iron emission line with interstellar/circumstellar absorption. The column density of the iron is varied as a free parameter, but the energy of the edge is fixed at 8.1 keV because we find that the fits are equally good for energies between 7.1 and 9.0 keV. For absorption, we assume neutral matter of solar abundance but exclude iron. The result of the fit is shown in Figure 4, and the parameters are summarized in Table 3. With model 3, an improved reduced χ^2 value of 1.24 is obtained, but the hydrogen column density determined from low-energy absorption is significantly lower than that inferred from the iron column density for the solar abundance (see § IVa). However, the level of the spectral dip around 10 keV is not very high compared with the systematic error in the background subtraction process. The structure around 3 keV in

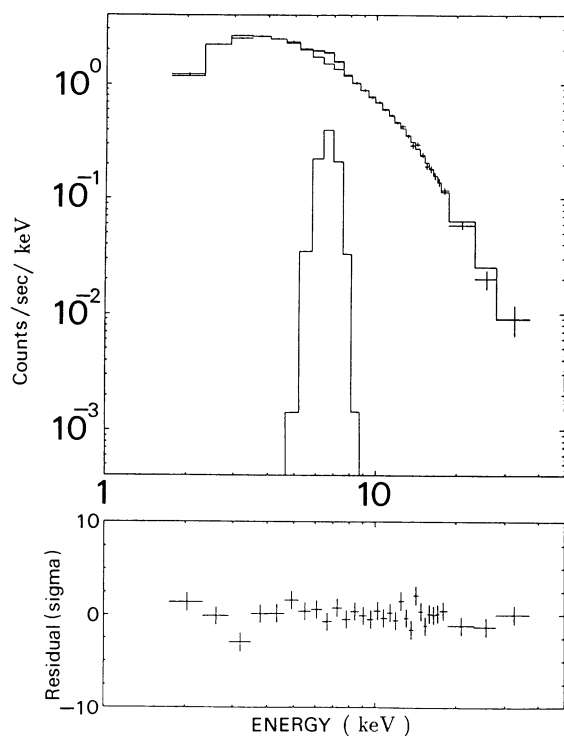


FIG. 4.—The flat-top spectrum fitted with model 3, which includes the iron edge.

Figure 3c, corresponding to the argon K-edge, is probably due to the relatively large systematic error in the background subtraction at this energy (Hayashida *et al.* 1989).

Finally, we have carried out phase-resolved spectral analysis at intervals of 0.125 in phase and examined the variation of the iron line. For this purpose we use model 1, since model 1 and model 3 give similar results for the iron line parameters (see Table 3), and the poorer statistics of each spectrum do not require the iron edge. Variations of the iron line parameters are shown in Figure 5. As clearly seen, the line intensity and equivalent width show positive correlation with the continuum intensity (Fig. 2a), whereas the line center energy stays constant at 6.6 ± 0.1 keV.

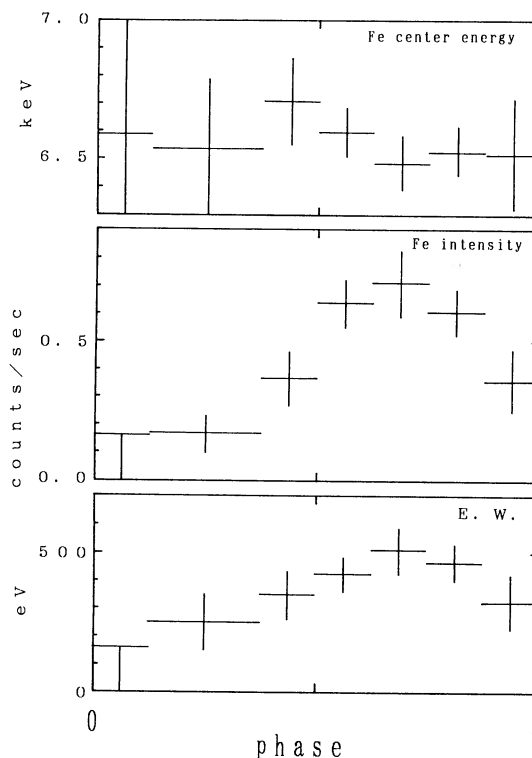


FIG. 5.—Phase-resolved spectral parameters for the iron emission line in the pulsing state. Phase zero epoch is the same as Figs. 2a and 2b. The line intensity and the equivalent width are modulated by the white dwarf rotation, whereas the line center energy stays constant.

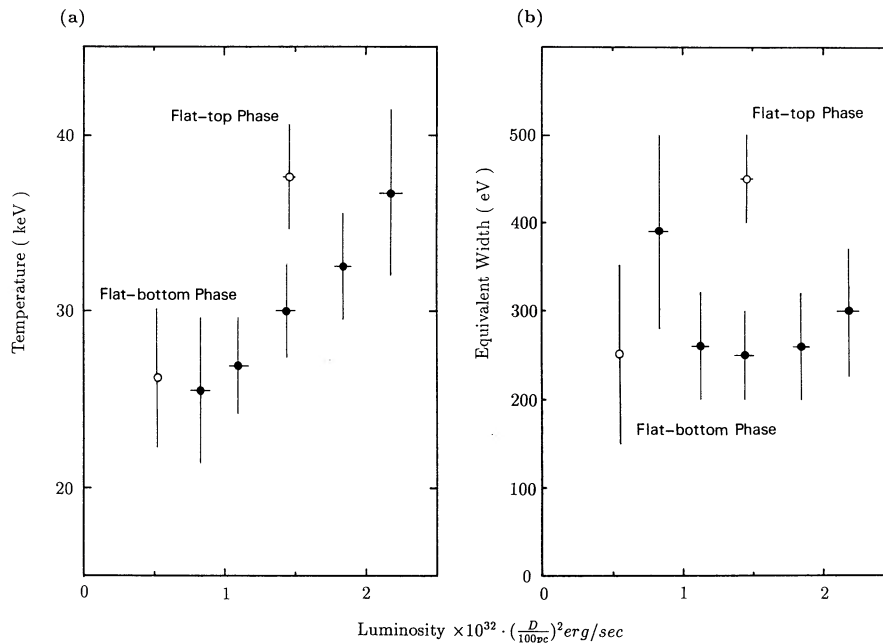


FIG. 6.—Spectral parameters in the flaring state: (a) relation between luminosity and temperature, and (b) relation between luminosity and the equivalent width of the iron line. Filled circles represent the data for the flaring state. For comparison the open circles represent the flat-bottom and the flat-top phases in the pulsing state.

d) Spectral Variation in the Flaring State

The data in the flaring state were sorted into five intensity groups in order to study spectral variations. Each spectrum is fitted with model 1, and the results are plotted in Figure 6.

The temperature of the emission region is roughly proportional to the source intensity (Fig. 6a). Also shown for comparison are the points corresponding to the flat-top and flat-bottom spectra taken from Table 3 (using model 1). The pulsing state shows qualitatively the same temperature variation with luminosity as the flaring state; however, the proportionality constant is larger by a factor of 2.

We also show the iron line equivalent width as a function of the source luminosity in Figure 6b. In the flaring state, the equivalent width can be regarded as constant at 250–300 eV, while in the pulsing state, the equivalent width is modulated due to the white dwarf rotation (see § IIIc).

IV. DISCUSSION

a) Continuum Spectra

Since the early theoretical work on emission mechanisms in magnetized cataclysmic variables, the hard X-ray flux has been thought to be generated through thermalization of kinetic energy at the shock front formed just above the white dwarf surface (Hoshi 1973; Aizu 1973; Fabian, Pringle, and Rees 1976; Kylafis and Lamb 1982; Frank, King and Lasota 1983). From the analyses presented above, this picture is confirmed for H0538+608. This is the third case (cf. AM Her [30.9 ± 4.5 keV; Rothschild *et al.* 1981] and EF Eri [18.1 ± 3.0 keV; Patterson, Williams, and Hiltner 1981]), in which the model is fully supported by the presence of a thermal X-ray spectrum with a temperature in excess of 10 keV. Furthermore, we find that the temperature varies as a function of pulse phase in the pulsing state, with a higher temperature during the flat-top phase. In the flaring state, the temperature of the emission region rises as the X-ray intensity increases.

In the pulsing state, an improved fit is obtained for the flat-top spectrum by incorporating the iron K-edge. We find that N_H obtained from the low-energy absorption is a factor of ~ 10 smaller than that inferred by the iron edge. This raises the possibility that some of the absorbing matter may be local to the binary and partially ionized due to a strong X-ray irradiation. To further investigate such a possibility, X-ray spectroscopy with substantially improved energy resolution would be needed.

b) Accretion-Pole Geometry

As shown in Figure 2a, the folded light curve of H0538+608 in the pulsing state exhibits a flat-top and a flat-bottom shape. The emission region is optically thin so that the observed intensity is a monotonically increasing function of the fractional volume of the emission region that can be seen by the observer (King and Shaviv 1984). We therefore consider that one emission region is periodically eclipsed and uncovered by the limb of the white dwarf. In addition, the substantial nonzero count rate in the flat-bottom phase compels us to postulate another X-ray emission region.

An accretion-pole geometry of H0538+608 was discussed by Mason, Liebert, and Schmidt (1989) based on their long-term optical polarimetry. In their circular polarimetry data, the sign of polarization stayed positive through some cycles, whereas it changed suddenly from plus to minus in other cycles. To explain these features, they introduced two accretion spots; one is always visible to the observer, while the other, with negative polarization, is periodically eclipsed by the limb of the white dwarf. The observed sudden change in the sign of circular polarization is interpreted as the appearance of the eclipsing spot from behind the limb of the white dwarf. To explain the cycle-to-cycle difference in the circular polarization behavior, they further assumed a flip-flop change in mass accretion rate between the two spots. Timing analysis of these

occasional sudden changes in polarization produced a tentative yet extremely precise ephemeris with a fractional error of 4×10^{-6} . In their interpretation, the phase is zero when the eclipsing spot comes into view.

Extrapolation of this tentative ephemeris forward to our epoch (4431 cycles) yields the phase of these polarization events (in our ephemeris) to be 0.34 ± 0.02 , which effectively marks the onset of the transition from the flat-bottom level to the flat-top level (Fig. 2a). This increase of the X-ray intensity also suggests the emergence of an accretion spot from behind the limb of the white dwarf. This coincidence between X-ray and optical polarimetry provides strong support with the accuracy of the tentative ephemeris of Mason, Liebert, and Schmidt (1989).

As for the geometry of these two accretion spots, however, it is possible that we observe completely different emission regions during the flat-top and the flat-bottom phases in the pulsing state, namely, two spots are alternatively eclipsed by the white dwarf. However, this cannot be the case in the flaring state. First, one may think that the pulse modulation could disappear if accreting mass goes into the two spots evenly. However, the observed X-ray intensity changes by a factor of three during the flaring state. This would require a new mechanism to balance the mass accretion rate between the two spots over this wide range of luminosity, and this mechanism must work only in the flaring state. Second, the pulse modulation may also disappear if the shock front becomes sufficiently high above the white dwarf surface so that the accretion spots are hardly eclipsed. However, this picture requires the shock height to be $\sim R_{\text{WD}}$, in contradiction to the theory ($\leq 0.1R_{\text{WD}}$: Aizu 1973; Frank, King, and Lasota 1983), hence considered to be highly unlikely.

c) The Iron Emission Line

The iron emission line can be used to investigate the structure of the emission region. Here we summarize the observed iron line behavior in the pulsing state (see Fig. 5):

1. The line center energy is kept at a constant value of 6.6 ± 0.1 keV through the white dwarf rotation. This energy corresponds to ionization states Fe xx–xxv if attributed to a single ionization state (Makishima 1986).

2. Both the equivalent width and the line intensity show maxima at the flat-top phase.

3. The equivalent width becomes as much as ~ 500 eV in the flat top phase.

These properties, in particular the spin modulation of the equivalent width, constrain the possible ion line emitter to the following four sites.

Site A.—Postshock region, whose temperature is ~ 30 keV. From this region, however, a 6.93 keV line with an equivalent width of about 120 eV is expected assuming ionization equilibrium.

Site B.—Preshock cool region.

Site C.—Surface of the white dwarf.

Site D.—Surface of the optical companion.

Here the iron line from site A is thermal emission from the hot plasma and those from sites B–D are fluorescence. From sites B–D we expect 6.4 keV lines from low ionized or neutral atoms. Among these candidates, site D can easily be rejected since the equivalent width and the line intensity should negatively correlate with the continuum intensity, as the heated surface and the X-ray source alternatively come into view.

The observed line center energy (6.6 ± 0.1 keV) implies either a thermal emission from a plasma with $kT \sim$ a few keV or a fluorescence by a cool matter with $\log \xi \sim 2.5$ (in units of cgs; Inoue 1985). Here, ξ is the ionization parameter defined as $\xi = L/nr^2$, with L , n , and r denoting the luminosity of the source, density of the fluorescing medium, and its distance from the source, respectively (Kallman and McCray 1982). The iron line is unlikely to be from a thermal plasma with $kT \sim$ a few keV because the continuum spectrum does not indicate such a component. In the case of fluorescence, the equivalent width of ~ 500 eV at the flat-top phase needs to be explained. For preshock cool matter, a column density of $\sim 3 \times 10^{23}$ cm^{-2} is required to produce an equivalent width of 500 eV, but it is much higher than that inferred from the observed low energy absorption. Albedo from the white dwarf surface ($N_{\text{H}} \sim 10^{24}$ cm^{-2}) can produce an equivalent width of about 3 keV if normalized by the scattered continuum (Inoue 1985). However, the X-ray reflectivity of the white dwarf surface at 6–7 keV is only ~ 0.2 , taking the ratio between absorption and scattering cross sections. Including the solid angle of the white dwarf, the expected equivalent width is not more than 300 eV compared with the direct continuum.

The difficulties would be overcome by combining sites A, B, and C, as first discussed by Swank, Fabian, and Ross (1984) based on the observation of AM Her. As shown above, combining sites A and C gives the equivalent width of ~ 400 eV. In addition, the preshock cool matter of $N_{\text{H}} \sim 10^{22}$ cm^{-2} can add an equivalent width of several tens of eV. So it is possible for the combination of these three components to produce enough iron emission. Taking this picture, the line center energy is calculated to be ~ 6.5 keV, in good agreement with the observation. These considerations suggest the mixture of thermal (6.9 keV) and fluorescent (6.4 keV) iron lines. To confirm this picture, we fitted the spectrum of the flat-top phase with model 3 but with two narrow emission lines with center energies 6.4 and 6.9 keV. The line intensities are varied as free parameters, and an acceptable χ^2 value of 1.2 is obtained.

d) The Temperature in the Flaring State

The mechanism of the hard X-ray emission in the flaring state probably remained the same as in the pulsing state, because the thermal bremsstrahlung model fits both states well. We find the temperature rises with X-ray luminosity (Fig. 6a). Shrader *et al.* (1988) report no correlation between X-ray hardness and intensity; however, the *EXOSAT* measurements are confined below ~ 10 keV. Some theoretical works (e.g., Aizu 1973; Frank, King, and Lasota 1983) predict a temperature that rises with mass accretion rates (although some models predict opposite sense; see Imamura and Durisen 1983). They assume that electrons are heated up to the maximum temperature at the shock front, and then they cool down through both bremsstrahlung and electron conduction as they descend in the accretion column. The higher mass accretion rate results in the shock to be formed closer to the white dwarf surface, hence giving higher temperature.

There is, however, another interpretation. In the shock front, almost all the energy is carried by ions because ions and electrons have the same velocity in the preshock region. Electrons are gradually heated up through Coulomb interaction with ions. The time scale of the energy transfer from ions to electrons is about the same order as the free fall time scale in the postshock region (Kuijpers and Pringle 1982), and the Coulomb interaction is an important process in determining

the hard X-ray spectrum. Since the energy transfer time scale is inversely proportional to the ion density, the electrons are heated up to higher temperature for higher mass accretion rate before landing on the white dwarf, in good agreement with the result shown in Figure 6a. But note that the discussion here needs further careful evaluation, especially concerning the efficiency of cooling mechanisms such as bremsstrahlung, electron conduction, and Compton cooling due to soft photons radiated from the white dwarf surface.

e) Mass of the White Dwarf

If the observed temperature, T_{obs} , is equal to the shock temperature, T_s , one can estimate the white dwarf mass using the theoretical relationship between the white dwarf mass and radius. However, there are reasons that T_s may be greater than T_{obs} (Fabian, Pringle, and Rees 1976; Kylafis and Lamb 1982; Imamura and Durisen 1983; Frank, King, and Lasota 1983):

1. The equipartition of internal energy may not be attained between ions and electrons.
2. The postshock electrons cool by thermal bremsstrahlung.
3. The thermal conduction from the shock front to the postshock region may not be negligible.
4. Compton scattering of the soft photons from the white dwarf surface may be effective.

Thus, only a lower limit to the white dwarf mass can be estimated. The highest temperature observed is 37.6 ± 3.0 keV for the flat-top phase in the pulsing state. From this,

$$M_{\text{WD}} \geq 0.71 M_{\odot} . \quad (1)$$

This relation is derived by assuming that the shock occurs on the surface of the white dwarf. An improved result could follow from optical spectroscopy and polarimetry (e.g., Mukai and Charles 1987).

V. CONCLUSIONS

The AM Her type source H0538 + 608 has been observed with *Ginga*. The results confirm that the hard X-ray spectrum can be described by thin thermal emission, supporting the existence of a standing shock. The behavior of H0538 + 608 changed in the middle of the observation. In the first half (pulsing state), modulation of the light curve caused by the

white dwarf rotation was clearly seen, whereas in the latter half (flaring state) it disappeared.

In the pulsing state the observed temperature (~ 38 keV) is higher than that of the other two AM Her type sources observed in X-rays, AM Her (30 keV: Rothschild *et al.* 1981) and EF Eri (18 keV: Patterson, Williams, and Hiltner 1981). In the flaring state, the temperature of the emission region increases with the mass accretion rate.

The X-ray pulsing state appears to require two active poles because (1) the X-ray spectra indicate optically thin thermal emission, (2) the folded X-ray light curves in the pulsing state have a flat-top and a flat-bottom shape, and (3) a substantial flux remains during the flat-bottomed region. The absence of periodicity in the flaring state further argues that one accretion spot is always in view; the accretion flow is directed primarily to this nonclipping pole during the flaring state. In this active 2-pole picture, previously put forward by Mason, Liebert, and Schmidt (1989) to explain their polarization data, the other pole is periodically eclipsed by the white dwarf. The polarization feature that represents the emergence of this eclipsing pole is in precise coincidence with the upward transition from the flat bottom to the flat top of the X-ray light curve, if their tentative, but very precise, ephemeris is adopted. This establishes with some confidence a physical connection between the X-ray and optical emission and provides support for their ephemeris.

Two cautionary notes are in order: (1) this scenario for the X-ray emission is based upon the interpretation that the folded X-ray light curve is truly flat-topped and flat-bottomed (i.e., the profile is not an artifact of the folding process); and (2) the optical spectroscopy and photometry obtained simultaneously with the X-ray data (to be published) indicate a more complex and time-dependent situation which requires additional detailed modeling.

A lower limit of the white dwarf mass is obtained by means of the maximum observed temperature. We obtain $\sim 0.7 M_{\odot}$ from the present observation.

The authors acknowledge support of the entire *Ginga* team in performing observations and data analysis. Support was provided by NASA (NAG8-691).

REFERENCES

- Aizu, K. 1973, *Progr. Theor. Phys.*, **49**, 1184.
 Beuermann, K., and Stella, L. 1985, *Space Sci. Rev.*, **40**, 139.
 Bonnet-Bidaud, J. M., and Mouchet, M. 1987, *Astr. Ap.*, **188**, 89.
 Cropper, M. 1990, *Space Sci. Rev.*, in press.
 Fabian, A. C., Pringle, J. E., and Rees, M. J. 1976, *M.N.R.A.S.*, **175**, 43.
 Forman, W., Jones, C., Cominski, L., Julien, P., Murray, S., Peters, G., Tananbaum, H., and Giacconi, R. 1978, *Ap. J. Suppl.*, **38**, 357.
 Frank, J., King, A. R., and Lasota, J.-P. 1983, *M.N.R.A.S.*, **202**, 183.
 Gould, R. J. 1980, *Ap. J.*, **238**, 1026.
 Hayashida, K., *et al.* 1989, *Pub. Astr. Soc. Japan*, **41**, 373.
 Heise, J., Brinkman, A. C., Gronenschild, E., Watson, M., King, A. R., Stella, L., and Kieboom, K. 1985, *Astr. Ap.*, **148**, L14.
 Hoshi, R. 1973, *Progr. Theor. Phys.*, **49**, 776.
 Imamura, J. N., and Durisen, R. H. 1983, *Ap. J.*, **268**, 291.
 Inoue, H. 1985, *Space Sci. Rev.*, **40**, 317.
 Kallman, T. R., and McCray, R. 1982, *Ap. J. Suppl.*, **50**, 263.
 King, A. R., and Shaviv, G. 1984, *M.N.R.A.S.*, **211**, 883.
 Kuipers, J., and Pringle, J. E. 1982, *Astr. Ap.*, **114**, L4.
 Kylafis, N. D., and Lamb, D. Q. 1982, *Ap. J. Suppl.*, **48**, 239.
 Lamb, D. Q. 1985, in *Low Mass X-Ray Binaries and Cataclysmic Variables*, ed. D. Q. Lamb and J. Patterson (Dordrecht: Reidel), p. 179.
 Makino, F., and the ASTRO-C Team 1987, *Ap. Letters Com.*, **25**, 223.
 Makishima, K. 1986, in *Lecture Notes in Physics*, Vol. **266**, *The Physics of Accretion onto Compact Objects*, ed. K. O. Mason, M. G. Watson, and N. E. White (Berlin: Springer-Verlag), p. 249.
 Mason, P. A., Liebert, J., and Schmidt, G. D. 1989, *Ap. J.*, **346**, 941.
 Morrison, R., and McCammon, D. 1983, *Ap. J.*, **270**, 119.
 Mukai, K., and Charles, P. A. 1987, *Ap. J.*, **226**, 209.
 Patterson, J., Williams, G., and Hiltner, W. A. 1981, *Ap. J.*, **245**, 618.
 Remillard, R. A., Bradt, H. V., McClintock, J. E., Patterson, J., Roberts, W., Schwartz, D. A., and Tapia, S. 1986, *Ap. J. (Letters)*, **302**, L11.
 Rothschild, R. E., *et al.* 1981, *Ap. J.*, **250**, 723.
 Shrader, C. R., Remillard, R., Silber, A., McClintock, J. E., and Lamb, D. Q. 1988, in *A Decade of UV Astronomy with the IUE Satellite* (ESA SP-281), Vol. 1, ed. E. J. Rolfe (Noordwijk: ESA), p. 137.
 Silber, A., Remillard, R., Bradt, H., Ishida, M., and Ohashi, T. 1990, in *Proc. 11th North American Workshop on CVs and LMB Systems*, ed. C. W. Mauche and F. Córdova (Cambridge: Cambridge University Press), in press.
 Stockman, H. S., Schmidt, G. D., and Lamb, D. Q. 1988, *Ap. J.*, **332**, 282.
 Swank, J. H., Fabian, A. C., and Ross, R. R. 1984, *Ap. J.*, **280**, 734.
 Turner, M. J. L., *et al.* 1989, *Pub. Astr. Soc. Japan*, **41**, 345.
 Wood, K., *et al.* 1984, *Ap. J. Suppl.*, **56**, 507.

H. V. BRADT, R. A. REMILLARD, and A. SILBER: Room 37-495, MIT, Cambridge, MA 02139

M. ISHIDA, K. MAKISHIMA, and T. OHASHI: Department of Physics, University of Tokyo, 7-3-1 Hongo, Bunkyo-ku, Tokyo 113, Japan